

Predictions for m_t and M_W in Minimal Supersymmetric Models

O. Buchmüller^a, R. Cavanaugh^{b,c}, A. De Roeck^{d,e}, J.R. Ellis^d, H. Flächer^f, S. Heinemeyer^g,
G. Isidori^{h,i}, K.A. Olive^j, F.J. Ronga^k, G. Weiglein^l

^aHigh Energy Physics Group, Imperial College, Blackett Lab., Prince Consort Road,
London SW7 2AZ, UK

^bFermi National Accelerator Laboratory, P.O. Box 500, Batavia, Illinois 60510, USA

^cPhysics Department, University of Illinois at Chicago, Chicago, Illinois 60607-7059, USA

^dCERN, CH-1211 Genève 23, Switzerland

^eAntwerp University, B-2610 Wilrijk, Belgium

^fDepartment of Physics and Astronomy, University of Rochester, Rochester, New York 14627, USA

^gInstituto de Física de Cantabria (CSIC-UC), E-39005 Santander, Spain

^hINFN, Laboratori Nazionali di Frascati, Via E. Fermi 40, I-00044 Frascati, Italy

ⁱInstitute for Advanced Study, T. U. München, Arcisstraße 21, D-80333 München, Germany

^jWilliam I. Fine Theoretical Physics Institute, Univ. of Minnesota, Minneapolis, Minnesota 55455, USA

^kInstitute for Particle Physics, ETH Zürich, CH-8093 Zürich, Switzerland

^lDESY, Notkestrasse 85, D-22603 Hamburg, Germany

Using a frequentist analysis of experimental constraints within two versions of the minimal supersymmetric extension of the Standard Model, we derive the predictions for the top quark mass, m_t , and the W boson mass, M_W . We find that the supersymmetric predictions for both m_t and M_W , obtained by incorporating all the relevant experimental information and state-of-the-art theoretical predictions, are highly compatible with the experimental values with small remaining uncertainties, yielding an improvement compared to the case of the Standard Model.

CERN-PH-TH/2009-223, DESY 09-207, FTPI-MINN-09/44, UMN-TH-2827/09

One of the most impressive successes of the Standard Model (SM) has been the accurate prediction of the mass of the top quark obtained from a fit to precision electroweak measurements at LEP and the SLC [1], which agrees very well with the value measured at the Tevatron [2]. To this may be added the equally successful prediction of the W mass [1,3]. The successes of these comparisons between theory and experiment re-

quire the incorporation of higher-order quantum corrections. In the SM these receive contributions from the postulated Higgs boson. Indeed, the precision data favour a relatively light Higgs boson weighing $\lesssim 150$ GeV [1].

One theoretical framework that predicts such a light Higgs boson is supersymmetry (SUSY) [4], which also possesses the ability to render more natural the electroweak mass hierarchy, contains

a plausible candidate for astrophysical dark matter, facilitates grand unification, and offers a possible explanation of the apparent discrepancy between the experimental measurement of the anomalous magnetic moment of the muon, $(g - 2)_\mu$, and the theoretical value calculated within the SM. There have been many analyses of the possible masses of particles within the minimal supersymmetric extension of the Standard Model (MSSM), taking into account the experimental, phenomenological and astrophysical constraints. For example, we have presented sparticle mass predictions [5,6,7] on the basis of a frequentist analyses of the relevant constraints in the context of simple models for SUSY breaking such as the CMSSM (in which the input scalar masses m_0 , gaugino masses $m_{1/2}$ and soft trilinear parameters A_0 are each universal at the GUT scale) and the NUHM1 (in which a common SUSY-breaking contribution to the Higgs masses is allowed to be non-universal). For an extensive list of references, see [7].

These analyses favour relatively light masses for the sparticles, indicating significant sensitivity of the precision observables to quantum effects of supersymmetric particles. It is therefore desirable to revisit the successful predictions of the SM, in particular the show-case predictions of m_t and M_W , to see how they are affected in the CMSSM and NUHM1. In particular, one may ask whether the SM prediction of m_t and M_W is improved, relaxed or otherwise altered in these models. The answer to this key question is non-trivial, since low-mass sparticles such as the \tilde{t} and \tilde{b} may contribute significantly to the prediction of electroweak observables [8], and the (lightest) Higgs mass is no longer an independent quantity, but also depends on the sparticle masses as we discuss below.

In this Letter, we make supersymmetric predictions for m_t and M_W within the same framework as our previous frequentist analyses of the CMSSM and NUHM1 parameter spaces [5,6,7]. The treatments of the experimental, phenomenological and astrophysical constraints are nearly identical with those in [7]. Here, we employ the updated SM value of $(g - 2)_\mu$ which includes a new set of low-energy e^+e^- data [9]. The new

value of $(g - 2)_\mu$ [10] does not significantly alter the regions of the CMSSM and NUHM1 parameter spaces favoured in our previous analyses.

Our statistical treatment of the CMSSM and NUHM1 makes use of a large sample of points (about 3×10^6) in the SUSY parameter spaces obtained with the Markov Chain Monte Carlo (MCMC) technique [11]. Our analysis is entirely frequentist, and avoids any ambiguity associated with the choices of Bayesian priors. The evaluations are performed using the **MasterCode** [5,6,7,12], which includes the following theoretical codes. For the RGE running of the soft SUSY-breaking parameters, it uses **SoftSUSY** [13], which is combined consistently with the codes used for the various low-energy observables: **FeynHiggs** [14,15,16] is used for the evaluation of the Higgs masses and a_μ^{SUSY} (see also [17,8]), for the other electroweak precision data we have included a code based on [18,19], **SuFla** [20,21] and **SuperIso** [22,23] are used for flavour-related observables, and for dark-matter-related observables **MicrOMEGAs** [24] and **DarkSUSY** [25] are used. In the combination of the various codes, **MasterCode** makes extensive use of the SUSY Les Houches Accord [26,27].

In the SM, the precision of the confrontation between theory and experiment is often expressed in the (m_t, M_W) plane. The experimental values of these quantities are essentially uncorrelated [1, 2,3],

$$m_t^{\text{exp}} = 173.1 \pm 1.3 \text{ GeV}, \quad (1)$$

$$M_W^{\text{exp}} = 80.399 \pm 0.023 \text{ GeV}, \quad (2)$$

shown in Fig. 1 as the black ellipse. In the SM, m_t is an independent input parameter, whereas the relation between the gauge boson masses M_W and M_Z can be predicted with high precision in terms of m_t , the Higgs mass, M_H^{SM} , and other model parameters, see [28] and references therein. The correlation between m_t and the prediction for M_W is displayed in Fig. 1 (foliated by lines of constant Higgs mass, M_H^{SM}).

A fit of the SM parameters to precision observables, e.g., those measured at the Z peak [29], yields indirect predictions for m_t and M_H^{SM} , and hence also a prediction for M_W . The SM predic-

tion for m_t without including the experimental limits on M_H^{SM} and ex- or including the experimental measurement of M_W is [1]

$$m_t^{\text{fit,SM,excl. } M_W} = 172.6_{-10.2}^{+13.3} \text{ GeV} , \quad (3)$$

$$m_t^{\text{fit,SM,incl. } M_W} = 179.3_{-8.5}^{+11.6} \text{ GeV} , \quad (4)$$

and the SM prediction for M_W , excluding the experimental measurement of M_W but either ex- or including the experimental measurement of m_t is [1]

$$M_W^{\text{fit,SM,excl. } m_t} = 80.363 \pm 0.032 \text{ GeV} , \quad (5)$$

$$M_W^{\text{fit,SM,incl. } m_t} = 80.364 \pm 0.020 \text{ GeV} . \quad (6)$$

The regions of the (m_t, M_W) plane favoured at the 68% C.L. by direct experimental measurements (1, 2) and in the SM fit (3, 5), shown as the dark (blue) contour [30] in Fig. 1 have significant overlap, representing a non-trivial success for the SM at the quantum level. However, we note that the overlap between the 68% C.L. contours happens in the region of Higgs mass values that are below the exclusion bound from the LEP SM Higgs searches, $M_H^{\text{SM}} > 114.4 \text{ GeV}$ [31], indicating a certain tension between the precision observables and the Higgs limit. Indeed, the experimental central value of M_W would be reached for a Higgs mass as low as $M_H^{\text{SM}} \sim 60 \text{ GeV}$. Combining the indirect measurements, m_t and M_W , the best-fit value of $M_H^{\text{SM}} \sim 87 \text{ GeV}$, and the 95% C.L. upper limit is $M_H^{\text{SM}} \sim 157 \text{ GeV}$ [1]. The direct searches at the Tevatron currently exclude a range $163 \text{ GeV} < M_H^{\text{SM}} < 166 \text{ GeV}$ [32], as also indicated by a white line in Fig. 1, so that the range $115 \text{ GeV} \lesssim M_H^{\text{SM}} \lesssim 150 \text{ GeV}$ is favoured in a global fit to the SM (including experimental bounds) at the 95% C.L. [33].

Turning now to our analysis in the case of supersymmetry, we note that the prediction for M_W as a function of m_t in the unconstrained MSSM gives rise to a band in Fig. 1 (shaded green) which has only little overlap (shaded blue) with the band showing the range of SM predictions for Higgs masses above the search limit from LEP. This is because the contribution of light supersymmetric particles tends to increase the predicted value of M_W compared to the SM case.

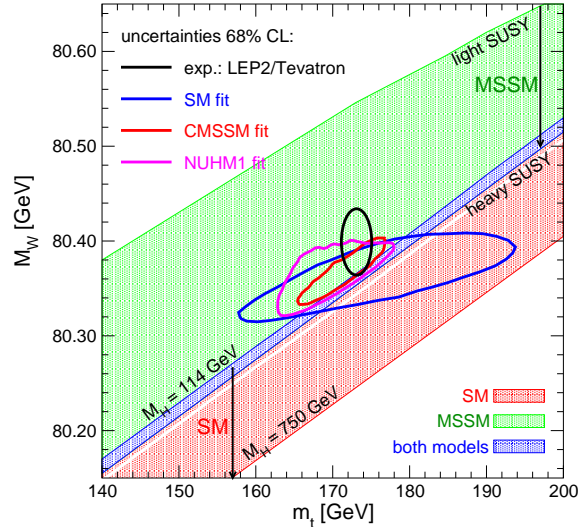


Figure 1. The 68% C.L. regions in the (m_t, M_W) plane predicted by a SM fit excluding the LEP Higgs constraint [1], and by CMSSM and NUHM1 fits including the LEP Higgs mass constraint, compared with the experimental measurements from LEP2 and the Tevatron shown as the black ellipse. The medium gray (red) and the dark (blue) shaded regions show the SM prediction, foliated by lines of constant M_H^{SM} values. The light gray (green) and the dark (blue) regions show the prediction of the unconstrained MSSM [18] ranging from light to heavy SUSY particles.

Furthermore, the overlap region (corresponding to the situation where all supersymmetric particles are heavy) is limited because, in contrast to the SM, the value of M_h is not an independent parameter in the MSSM, but is calculable in terms of the sparticle masses with an upper limit $\sim 135 \text{ GeV}$ [15].

We have performed fits in the CMSSM and the NUHM1 including all relevant experimental information as specified in [7], i.e., we include all precision observables used in the SM fit shown in Fig. 1 (except Γ_W , which has a minor impact) as well as constraints from $(g-2)_\mu$, flavour physics, the cold dark matter (CDM) relic density and

the direct searches for the Higgs boson and supersymmetric particles. The direct experimental measurements of M_W and m_t , on the other hand, have *not* been included in these global fits. The results of our fits in the CMSSM and the NUHM1 are also displayed as 68% C.L. contours in Fig. 1, and show remarkably good agreement with the experimental measurements of M_W and m_t .

The 68 and 95% C.L. regions in the (m_t, M_W) plane found in the CMSSM (NUHM1) fit are shown in more detail in the upper (lower) panel of Fig. 2. The fits within the MSSM differ from the SM fit in various ways. First, the number of free parameters is substantially larger in the MSSM, even restricting ourselves to the CMSSM and the NUHM1. On the other hand, more observables are included in the fits, providing extra constraints. We recall that in the SM fits $(g-2)_\mu$ and the B -physics observables have a minor impact on the best-fit regions, and are not included in the results shown above, which are taken from [1] (see e.g. [34] for an alternative approach), while the relic density of CDM cannot be accommodated in the SM. Furthermore, as already noted, whereas the light Higgs boson mass is a free parameter in the SM, it is a function of the other parameters in the CMSSM and NUHM1. In this way, for example, the masses of the scalar tops and bottoms enter not only directly into the prediction of the various observables, but also indirectly via their impact on M_h . This provides additional motivation for including the experimental constraints on M_h into the fits in the MSSM.

In Fig. 3, we show the results of the same fit as in Fig. 2, but now in the (M_h, m_t) plane for the CMSSM (NUHM1) in the upper (lower) panel. The LEP lower limit of 114 GeV is applicable in the CMSSM [35,36], but cannot always be directly applied in the NUHM1, since there are regions of the NUHM1 parameter space where the hZZ coupling is suppressed relative to its value in the SM [37]. We use the prescription given in [7] to calculate the $\chi^2(M_h)$ contribution for points with suppressed hZZ couplings, and see in the lower panel of Fig. 3 a significant set of NUHM1 points with $M_h \ll 114$ GeV: these reflect the shape of the $\Delta\chi^2$ function in the right panel of

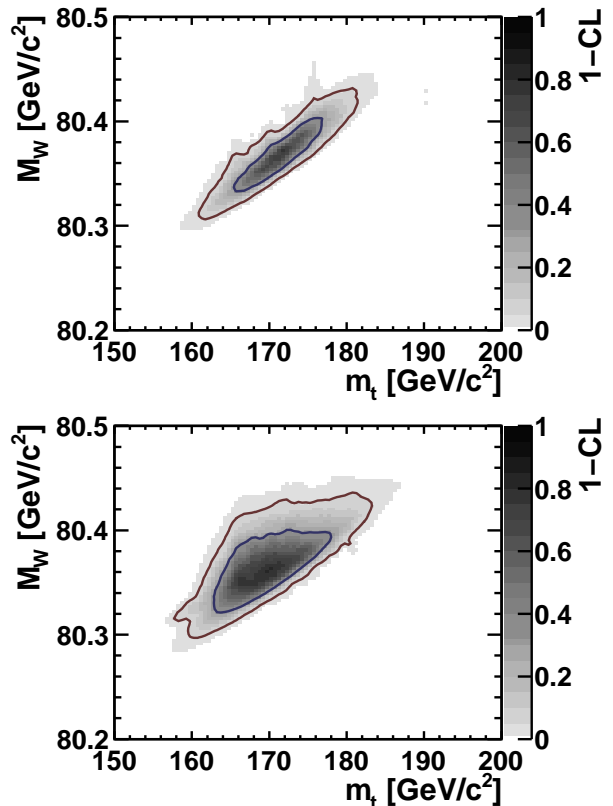


Figure 2. The 68% and 95% C.L. regions in the (m_t, M_W) planes for the CMSSM (upper) and for the NUHM1 (lower), for fits that do not include the direct measurements of m_t and M_W , but do incorporate the appropriate LEP constraint on M_h .

Fig. 4 of [7]. The appearance of a local minimum at $M_h \approx 100$ GeV in the lower plot of Fig. 3 is statistically not significant. It sensitively depends on the details of the implementation of the Higgs search bounds.

We now turn to the single-variable χ^2 functions for m_t and M_W . In the upper panel of Fig. 4, we show the χ^2 functions for m_t in the CMSSM and NUHM1 as solid and dashed lines respectively with M_W included in the fit (as before, the direct measurement of m_t is not included in this

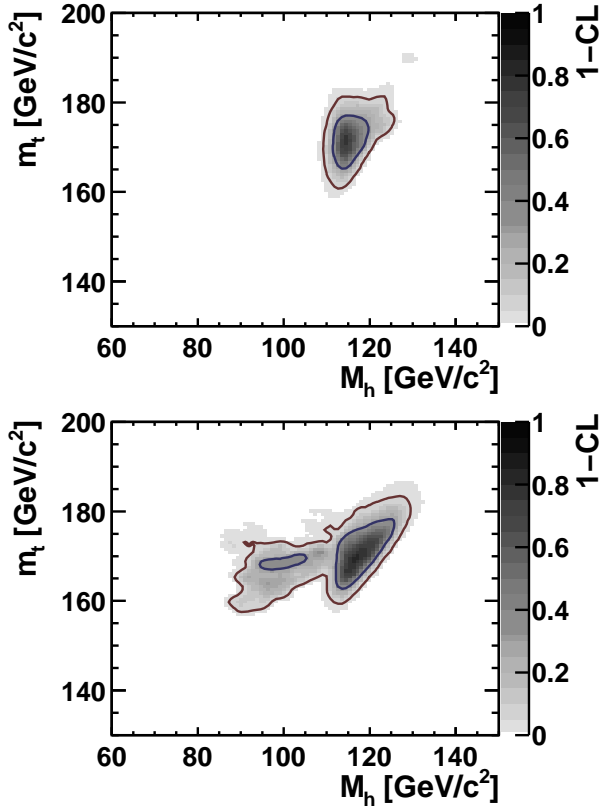


Figure 3. The 68% and 95% C.L. regions in the (M_h, m_t) planes for the CMSSM (upper plot) and for the NUHM1 (lower plot), for fits that do not include the direct measurements of m_t and M_W , but do incorporate the appropriate LEP constraint on M_h .

fit). Comparing the results with the SM fit, we find that these rise more sharply, in particular for larger values of m_t , than they would in the SM fit, indicating that the upper bound on m_t from the indirect prediction in the MSSM is significantly reduced compared to the SM case. We find the 68% C.L. ranges

$$m_t^{\text{fit,CMSSM,incl. } M_W} = 173.8_{-3.1}^{+3.2} \text{ GeV}, \quad (7)$$

$$m_t^{\text{fit,NUHM1,incl. } M_W} = 169.5_{-3.4}^{+8.8} \text{ GeV}. \quad (8)$$

Comparing with the SM fit result (4), we find

lower central values for m_t in both the CMSSM and NUHM1 in better agreement with the experimental result (1). The reduction in the upper bound on m_t reflects, in particular, the fact that the additional contribution from the \tilde{t} and \tilde{b} enters with the same sign as the leading SM-type contribution to the precision observables that is proportional to $m_{\tilde{t}}^2$. A non-vanishing contribution from superpartners therefore tends to reduce the preferred value of m_t compared to the SM fit. It should be noted in this context that the smaller uncertainties in m_t found in the supersymmetric fits compared to the SM case (particularly in the CMSSM) can in part also be attributed to the fact that a larger set of observables has been used in the CMSSM and NUHM1 fits.

For the W boson mass, we find the χ^2 functions including m_t in the fit in the CMSSM (solid) and NUHM1 (dashed) shown in the lower panel of Fig. 4, and the corresponding 68% C.L. ranges

$$M_W^{\text{fit,CMSSM,incl. } m_t} = 80.379_{-0.014}^{+0.013} \text{ GeV}, \quad (9)$$

$$M_W^{\text{fit,NUHM1,incl. } m_t} = 80.370_{-0.011}^{+0.024} \text{ GeV}. \quad (10)$$

The best-fit values of these predictions are substantially higher than the SM prediction (6) based on precision electroweak data (in particular in the CMSSM) and are closer to the experimental value (2), again with smaller uncertainties.

We summarize our main results in Fig. 5. The upper (lower) panel compares the experimental measurement of m_t (M_W) with the predictions of a SM fit to precision electroweak data and our final predictions in the CMSSM and NUHM1. The resulting agreement of the final predictions for m_t with the experimental value (1) is remarkable, almost embarrassingly good in the CMSSM case, and very good in the NUHM1. Compared to the SM fit, the best-fit values for M_W in the CMSSM and NUHM1 are closer to the experimental value (2), and in the CMSSM case the best-fit value lies within the experimental 68% C.L. range. We conclude that the CMSSM and NUHM1 pass with flying colours the test of reproducing the successful SM predictions of m_t and M_W , even improving on them. We can only hope that this probe of SUSY at the loop level will soon be made even more precise with the discovery of sparticles at

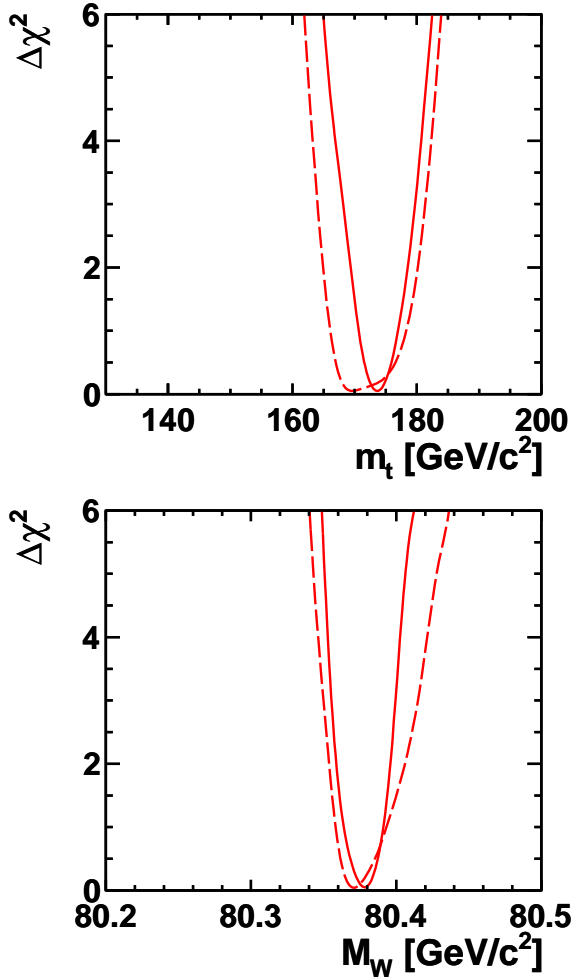


Figure 4. The χ^2 functions for m_t (upper panel) in the CMSSM (solid) and NUHM1 (dashed) excluding the direct m_t mass measurement but including all the other experimental information. The corresponding χ^2 functions for M_W (lower panel) excluding the direct M_W mass measurement but again including all the other experimental information.

the LHC.

This work was supported in part by the European Community's Marie-Curie Research Training Network under contracts MRTN-CT-2006-

035505 'Tools and Precision Calculations for Physics Discoveries at Colliders' and MRTN-CT-2006-035482 'FLAVIANet', and by the Spanish MEC and FEDER under grant FPA2005-01678. The work of S.H. was supported in part by CI-CYT (grant FPA 2007-66387), and the work of K.A.O. was supported in part by DOE grant DE-FG02-94ER-40823 at the University of Minnesota.

REFERENCES

1. LEP Electroweak Working Group, <http://lepewwg.web.cern.ch>.
2. Tevatron Electroweak Working Group and CDF Collaboration and D0 Collaboration, arXiv:0903.2503 [hep-ex].
3. Tevatron Electroweak Working Group, arXiv:0908.1374 [hep-ex].
4. H. E. Haber and G. L. Kane, Phys. Rept. **117** (1985) 75.
5. O. Buchmueller *et al.*, Phys. Lett. B **657** (2007) 87 [arXiv:0707.3447 [hep-ph]].
6. O. Buchmueller *et al.*, JHEP **0809** (2008) 117 [arXiv:0808.4128 [hep-ph]].
7. O. Buchmueller *et al.*, Eur. Phys. J. C **64** (2009) 391 [arXiv:0907.5568 [hep-ph]].
8. S. Heinemeyer, W. Hollik and G. Weiglein, Phys. Rept. **425** (2006) 265 [arXiv:hep-ph/0412214].
9. B. Aubert *et al.* [The BABAR Collaboration], arXiv:0908.3589 [hep-ex].
10. M. Davier, A. Hoecker, B. Malaescu, C. Z. Yuan and Z. Zhang, arXiv:0908.4300 [hep-ph].
11. The analysis in [5,6,7], on which this paper is based, involved thorough samplings of CMSSM and NUHM1 mass parameters out to several TeV, which included the rapid-annihilation funnel and focus-point regions, as well as the coannihilation region. The fact that the latter region is favoured in our analysis is *not* a sampling artifact, but is related directly to the different contributions to the overall χ^2 function of several observables, notably $(g-2)_\mu$, as documented in Table 2 and the text of [7].
12. See <http://cern.ch/mastercode>.

13. B. C. Allanach, *Comput. Phys. Commun.* **143** (2002) 305 [arXiv:hep-ph/0104145].
14. S. Heinemeyer, W. Hollik and G. Weiglein, *Comput. Phys. Commun.* **124** (2000) 76 [arXiv:hep-ph/9812320]; *Eur. Phys. J. C* **9** (1999) 343 [arXiv:hep-ph/9812472]. See <http://www.feynhiggs.de>.
15. G. Degrandi *et al.*, *Eur. Phys. J. C* **28** (2003) 133 [arXiv:hep-ph/0212020].
16. M. Frank *et al.*, *JHEP* **0702** (2007) 047 [arXiv:hep-ph/0611326].
17. T. Moroi, *Phys. Rev. D* **53** (1996) 6565 [Erratum-ibid. *D* **56** (1997) 4424] [arXiv:hep-ph/9512396].
18. S. Heinemeyer *et al.*, *JHEP* **0608** (2006) 052 [arXiv:hep-ph/0604147].
19. S. Heinemeyer, W. Hollik, A. M. Weber and G. Weiglein, *JHEP* **0804** (2008) 039 [arXiv:0710.2972 [hep-ph]].
20. G. Isidori and P. Paradisi, *Phys. Lett. B* **639** (2006) 499 [arXiv:hep-ph/0605012].
21. G. Isidori, F. Mescia, P. Paradisi and D. Temes, *Phys. Rev. D* **75** (2007) 115019 [arXiv:hep-ph/0703035], and references therein.
22. F. Mahmoudi, *Comput. Phys. Commun.* **178** (2008) 745 [arXiv:0710.2067 [hep-ph]]; *Comput. Phys. Commun.* **180**, 1579 (2009) [arXiv:0808.3144 [hep-ph]].
23. D. Eriksson, F. Mahmoudi and O. Stal, *JHEP* **0811** (2008) 035 [arXiv:0808.3551 [hep-ph]].
24. G. Belanger, F. Boudjema, A. Pukhov and A. Semenov, *Comput. Phys. Commun.* **176** (2007) 367 [arXiv:hep-ph/0607059]; *Comput. Phys. Commun.* **149** (2002) 103 [arXiv:hep-ph/0112278]; *Comput. Phys. Commun.* **174** (2006) 577 [arXiv:hep-ph/0405253].
25. P. Gondolo *et al.*, *New Astron. Rev.* **49** (2005) 149; *JCAP* **0407** (2004) 008 [arXiv:astro-ph/0406204].
26. P. Skands *et al.*, *JHEP* **0407** (2004) 036 [arXiv:hep-ph/0311123].
27. B. Allanach *et al.*, *Comput. Phys. Commun.* **180** (2009) 8 [arXiv:0801.0045 [hep-ph]].
28. M. Awramik, M. Czakon, A. Freitas and G. Weiglein, *Phys. Rev. D* **69** (2004) 053006 [arXiv:hep-ph/0311148].
29. [ALEPH Collaboration and DELPHI Collaboration and L3 Collaboration and OPAL Collaboration], *Phys. Rept.* **427** (2006) 257 [arXiv:hep-ex/0509008].
30. http://lepewwg.web.cern.ch/LEPEWWG/plots/summer2009/s09_mt_mw_contours.eps.
31. R. Barate *et al.* [ALEPH, DELPHI, L3, OPAL Collaborations and LEP Working Group for Higgs boson searches], *Phys. Lett. B* **565** (2003) 61 [arXiv:hep-ex/0306033].
32. [CDF Collaboration and D0 Collaboration], arXiv:0911.3930 [hep-ex].
33. H. Flacher *et al.*, *Eur. Phys. J. C* **60** (2009) 543 [arXiv:0811.0009 [hep-ph]], see: <http://www.cern.ch/gfitter>.
34. C. Amsler *et al.* [Particle Data Group], *Phys. Lett. B* **667** (2008) 1.
35. J. R. Ellis, S. Heinemeyer, K. A. Olive and G. Weiglein, *Phys. Lett. B* **515** (2001) 348 [arXiv:hep-ph/0105061].
36. S. Ambrosanio *et al.*, *Nucl. Phys. B* **624** (2002) 3 [arXiv:hep-ph/0106255].
37. S. Schael *et al.* [ALEPH, DELPHI, L3, OPAL Collaborations and LEP Working Group for Higgs boson searches], *Eur. Phys. J. C* **47** (2006) 547 [arXiv:hep-ex/0602042].

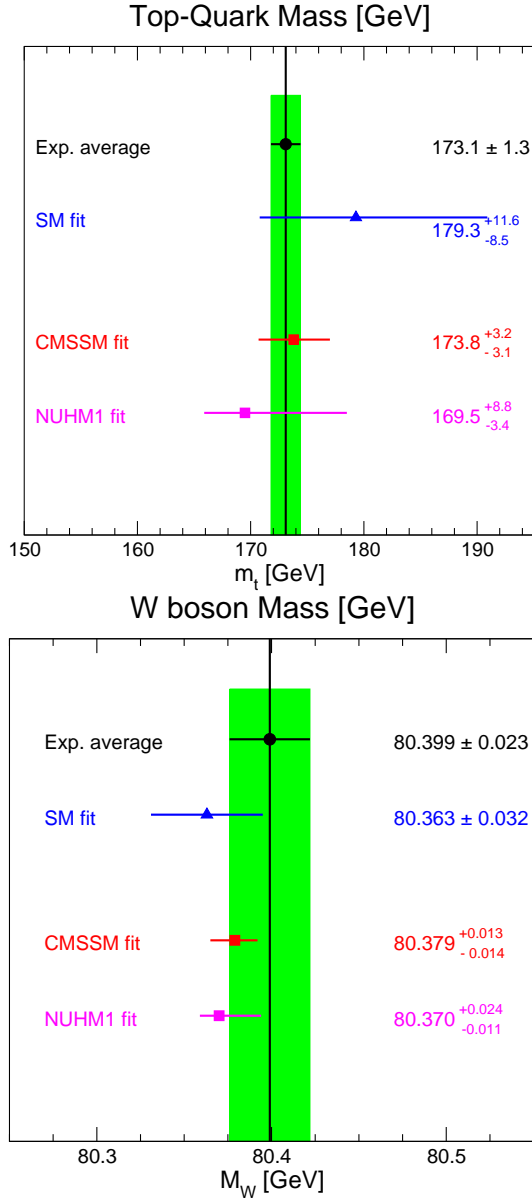


Figure 5. The 68% C.L. ranges for m_t (upper panel) and M_W (lower panel) including (from top to bottom) the experimental average, and the predictions of the SM (not incl. the M_H^{SM} limits) [1], CMSSM and NUHM1 fits, using all the available information except the direct mass measurement.